

Diazocine Derivatives: A Family of Azobenzenes for Photochromism with Highly Enhanced Turn-On Fluorescence

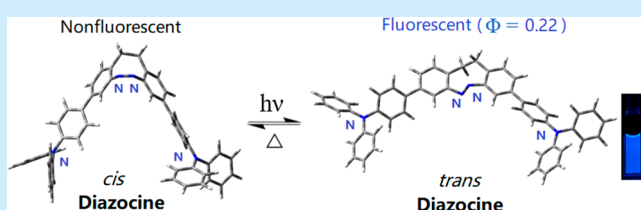
Qian Zhu,[†] Suning Wang,^{†,‡,✉} and Pangkuan Chen^{*,†,✉}

[†]Beijing Key Laboratory of Photoelectronic/Electrophotonic Conversion Materials, Key Laboratory of Cluster Science of the Ministry of Education, School of Chemistry and Chemical Engineering, Beijing Institute of Technology of China, Beijing 102488, People's Republic of China

[‡]Department of Chemistry, Queen's University, Kingston, Ontario K7L 3N6, Canada

S Supporting Information

ABSTRACT: π -Conjugated azobenzene derivatives were reported to couple azo moieties with aryl fluorophore. Using the photochemistry of the C_2 -bridged azobenzene, we have accomplished two diazocine-based photoswitching molecules (**cAz1** and **cAz2**). In addition to remarkable photochromic properties, they show a turn-on fluorescence, and the emission was highly enhanced with quantum efficiency increasing up to 0.22 for **cAz1**. The emission remains persistent and can only be switched off via thermal deactivation. They display greater optical responses, compared with the linear analogues (**Az1**–**Az4**). This work may provide a new scaffold toward advanced light-emitting materials using photoswitchable systems.



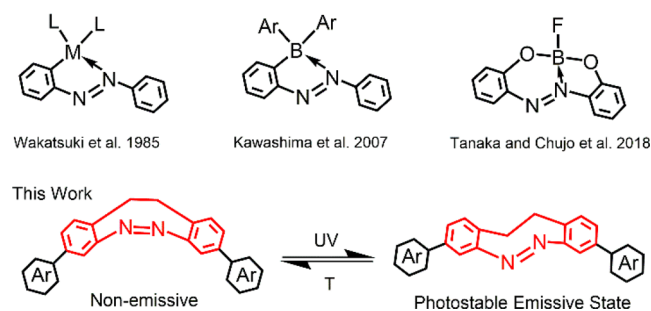
Photochromic molecular systems represent an important class of stimuli-responsive materials and have gained tremendous attention for broad applications in optical sensors, memories, and photoswitching devices.^{1–3} These molecules reversibly switch configurations between their isomers, leading to distinct color change concomitant with photoisomerization processes modulated by the key photoswitchable functionality. Among components of this type, the dyes of azobenzene and derivatives have been well-established as being the most frequently utilized photochromic compounds, because of easier access and highly controllable photochemistry, compared to some other counterparts.^{4–11} They usually undergo a very efficient and reversible *cis*–*trans* photoconversion upon exposure to UV-vis light irradiation, leading to optical characteristics in the photophysical absorption.

Diazocines, which are new derivatives of azobenzene bridged by ethylene in the ortho positions, were developed by Siewertsen et al. for further improved photoswitching behavior.¹² As unconventional cyclic azobenzene motifs, diazocines have been convinced that the large separation (~85 nm) of n – π^* transitions in the absorption bands for the *cis* and *trans* isomers is intrinsically ascribed to the geometrical ring constraints.^{6,13} The unique ring structure of diazocines plays a key role in pursuing excellent photochemical efficiency, and quantitative photoconversions were achieved between the two configurations. Very recently, heterodiazocines (e.g., O- and S-diazocines) were also reported to unveil new photochemistry in the literature.¹⁴

However, the photochromic switching of azobenzene generally proceeds at the expense of photoluminescence capability, since the ultrafast nonradiative photoisomerization

of the N=N bond on a picosecond time scale can deactivate the excited fluorophore.¹⁵ Consequently, the universal design principle applied to azo-based luminescent materials remains considerably elusive. To date, several limited pathways have been proposed for azobenzene luminescence, such as the formation of $X \leftarrow N=N$ coordination bonds ($X = B, Si, M$; see Scheme 1),^{16–18} self-assembled chromophore aggrega-

Scheme 1. Selected Systems of Strong Fluorescent Azobenzene Derivatives



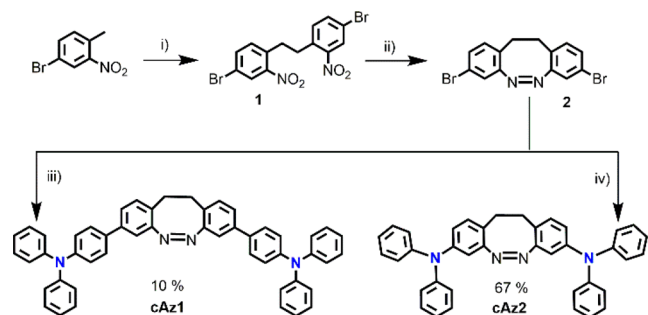
tion,¹⁹ and decoupling fluorescence mechanism.²⁰ However, azobenzene-based systems that emit intense luminescence without shutdown of the photoswitching properties are fundamentally important for new light-emitting materials. Herein, we first describe the synthetic strategy of diazocine-based conjugated luminescent materials using the ring-

Received: April 6, 2019

constrained molecular systems. We expect these compounds might be considered as advanced photoswitchable emitters, because their luminescence behavior could be switched at no expense of the photochromic properties upon *cis*–*trans* isomerizations.

The synthetic procedures for **cAz1**, **cAz2**, and **Az1**–**Az4** are shown in Scheme 2 and Supporting Information (SI),

Scheme 2. Synthetic Route of **cAz1** and **cAz2**^a



^aReagents and conditions: (i) *t*-BuOK, Br₂ (1.3 equiv), THF, 0 °C, 12 h; (ii) zinc powder, Ba(OH)₂ (4.0 equiv), EtOH/H₂O, reflux, 200 min; (iii) 4-Ph₂NC₆H₄SnMe₃ (2.0 equiv), Pd(PPh₃)₄, toluene, reflux, 12 h, under N₂; and (iv) diphenylamine (2.5 equiv), Pd(OAc)₂ (5% mol), Xantphos (5% mol), *t*-BuONa, toluene, reflux, 12 h, under N₂.

respectively. We started the synthesis of diazocines by the homocoupling reaction of 4-bromo-1-methyl-2-nitrobenzene to give compound **1** in the presence of Br₂ under basic conditions. Subsequently, the core building block **2** was obtained via intramolecular reductive cyclization of the resulting C₂-bridged intermediate in dilute basic solutions of EtOH/H₂O. Next, the Pd-catalyzed Stille and Buchwald coupling reactions of **2** and aryl amines under standard conditions led to products of **cAz1** and **cAz2**, respectively. As detailed in the SI, the Suzuki coupling of (*E*)-1,2-bis(3-iodophenyl)diazene with Ar₃N- or Ar₃B-substituted borane moieties resulted in the linear azobenzene derivatives **Az1** and **Az3** (see structures in Figure 1). Similarly, two other analogues

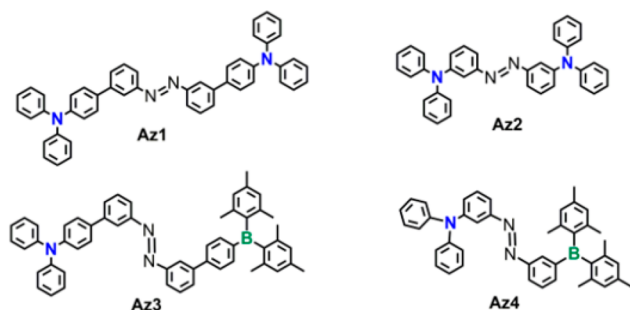


Figure 1. Structures of N- and B-functionalized π -conjugated azo compounds.

Az2 and **Az4** were prepared through Buchwald C–N coupling reactions. These molecules were fully characterized by nuclear magnetic resonance (¹H, ¹³C, and ¹¹B NMR) and high-resolution mass spectroscopy (HRMS) spectroscopic analyses.

The solid-state structures of **cAz1**, **Az1**, and **Az2** were examined by single-crystal X-ray diffraction (XRD) analysis. The crystals of **cAz1** were obtained by slow evaporation from the solution of dichloroethane/methanol (DCE/MeOH). As

shown in Figure 2a, **cAz1** displays a bow-shaped ribbon structure in good agreement with density functional theory

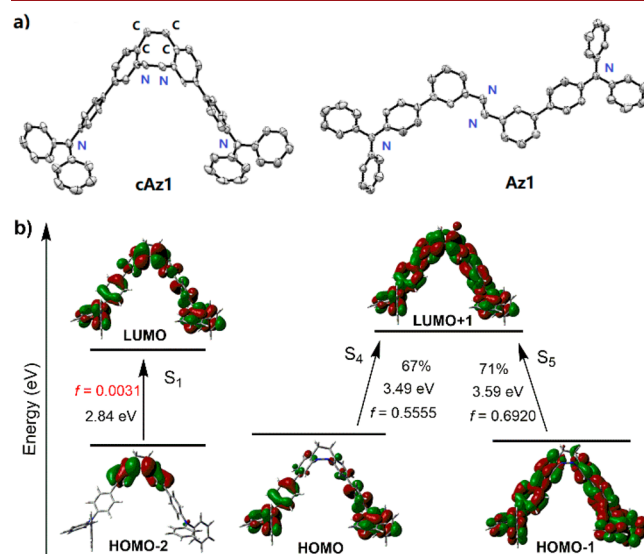


Figure 2. (a) Single-crystal X-ray structures of **cAz1** and **Az1**. H atoms and solvent molecules are omitted. (b) Vertical excitation energy (eV), oscillator strength (*f*), and key orbitals involved in transitions to S₄ and S₅ states (isovalue = 0.02, TD-DFT, B3LYP/6-311G**) for **cAz1**-Z.

(DFT) computations for the Z isomer that is thermodynamically more stable than the E isomer, because of the ring constraint of ethylene bridge.^{11–13} The highly curved cyclic unit leads to a bending angle ($\sim 73.7^\circ$) between the two moieties determined by the Ph rings of diazocines (see the SI). The CNNC moiety is almost coplanar with a slight twist of $\sim 7.4^\circ$ and NNC angles of $\sim 120^\circ$. While the CCCC moiety deviates from planarity with a pronounced torsion angle of $\sim 36.5^\circ$, leading to some configurational flexibility required for further photoisomerization. The N=N bond length of 1.265(6) Å was found to be much shorter than that of 1.531(8) Å for C–C single bond of the C₂ bridge (Figure S28 in the SI). In contrast, the linear analogues of **Az1** and **Az2** show E isomeric crystal structures (Figure 2a (right) and the SI), consistent with those commonly observed in parent azobenzenes.

DFT and time-dependent density functional theory (TD-DFT) calculations (B3LYP, 6-31G*, and 6-311G**) were performed, and the results are summarized in the SI. Once aryl substituents are coupled with azobenzene moieties, the HOMO energy levels are strongly increased from -6.11 eV for the model to approximately -4.95 eV for **cAz1**, **cAz2**, and **Az1**–**Az4**, and the HOMO–LUMO energy gaps are hence squeezed (Table S5 in the SI). For **cAz1** and **cAz2**, the lowest unoccupied molecular orbital (LUMO) levels are reduced by ~ 0.2 eV as the configurations are switched from the Z-isomer to the E-isomer, leading to a stronger electron-accepting diazocine functionality, together with a red-shifted optical excitation by 50 nm. **cAz1**-Z shows the highest occupied molecular orbital (HOMO) mainly localized on terminal Ar₃N moieties, while the LUMO is fully delocalized over the π -conjugated system involving diazocines and the N moieties (Figure 2b). However, the stretched **cAz1**-E isomer has a less efficient π -conjugation of the HOMO and LUMO (Figure S43 in the SI). Vertical excitations to the S₁, S₂, and S₃ states have

similar energies and weak oscillator strengths, and other transitions are likely much more effective (Table S7 in the SI). As a representative example, **cAz1** shows the $n-\pi^*$ transition to S_4 (HOMO \rightarrow LUMO+1, 356 nm, 3.49 eV, $f = 0.5555$) and $\pi-\pi^*$ transition to S_5 state (HOMO-1 \rightarrow LUMO+1, 346 nm, 3.59 eV, $f = 0.6920$) (Figure 2b; also see Table S6 in the SI).

To explore the switchable photochromic properties, the photophysical behaviors of these compounds were investigated by UV-vis absorption and ^1H NMR spectroscopy (see Figures 3 and 4, as well as Figures S29–S35 in the SI). Solutions of

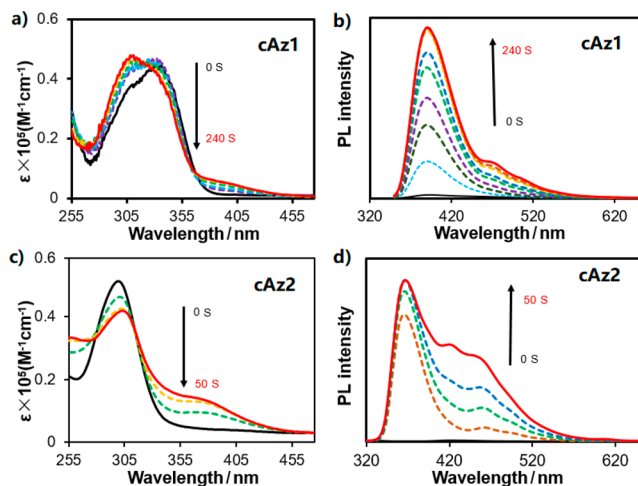


Figure 3. Absorption and photoluminescence (PL) spectral change of (a,b) **cAz1** and (c,d) **cAz2** upon irradiation under UV light ($\lambda = 300$ nm) in THF ($c = 1.0 \times 10^{-5}$ M, $\lambda_{\text{ex}} = \lambda_{\text{abs(max)}}$).

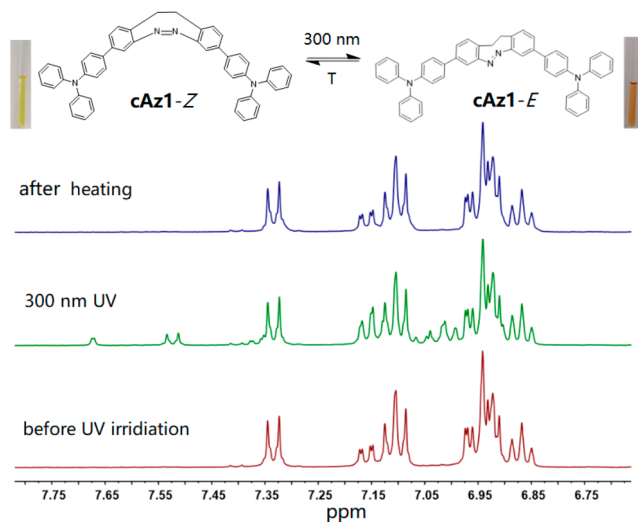


Figure 4. Comparison of aromatic ^1H NMR signals of **cAz1** between the *cis* and *trans* isomers on exposure to the UV light ($\lambda = 300$ nm) and thermal recovery in 10 min. Inset photographs show photochromic visualization of solutions.

cAz1 and **cAz2** are light yellow under ambient conditions. Upon UV irradiation at 300 nm, the colors turn dark brown, because of the forward photoisomerization. The THF solution of **cAz1** shows a decrease in the strong $n-\pi^*$ transition at $\lambda = 336$ nm, together with an increase in the bathochromically shifted absorption at $\lambda = 386$ nm. This features the typical switching for the $Z \rightarrow E$ isomerization of diazocines.¹² In addition, the $\pi-\pi^*$ excitation is further enhanced around 310

nm in the *E* configuration (Figure 3a). Similar spectral changes were observed for **cAz2** but with an even faster isomerization, within 50 s, in comparison to **cAz1** and **Az1–Az4** (see Figure 3b, as well as Figure S29 in the SI). Surprisingly, under the visible light irradiation at 410 nm, the **cAz1-E** isomer was found to be highly photochemically stable without significant changes in absorption and ^1H NMR signals. Alternatively, the back conversion to the *Z* isomers can be accomplished for **cAz1** and **cAz2** upon heating to ~ 70 °C in 10 min. The full recovery of *Z* configurations was confirmed by ^1H NMR studies (see Figure 4 and the SI). They behave distinctively from the photoreversible parent diazocines and heterodiazocines reported previously,^{12,14} which may be attributed to the electronic stabilization via π -conjugation. The photoisomerization efficiencies (Φ_{conv}) were acquired from the UV-vis absorbance determined at the photostationary state of THF solutions and are summarized in Table 1. Compared with parent molecules, the relatively small photoconversion from 14% to 46% could also be induced by π -extension of the conjugated skeleton.

Table 1. Summary of the Absorption, Photoluminescence (PL), and Fluorescence Quantum Efficiency (Φ)

	λ_{abs}^a (nm)	λ_{abs}^b (nm)	λ_{PL}^b (nm)	Φ_{PL}^a (%)	Φ_{PL}^b (%)	τ_{av}^b (ns)	Φ_{conv}^c (%)
cAz1	336	335, 386	390	<1	22	1.9	14
cAz2	300	300, 380	366, 461	<1	6	2.5	19
Az1	328	327, 388	394	<1	14	1.3	14
Az2	302	302, 368	362	1.0	9	5.5	39
Az3	331	331, 393	390, 488	<1	8	3.7	18
Az4	311	310, 375	363, 472	1.0	16	7.4	46

^aRecorded in THF ($c = 1.0 \times 10^{-5}$ M) before irradiation under UV light ($\lambda = 300$ nm). ^bRecorded after UV irradiation. λ_{abs} and λ_{PL} are shown with maximum values. ^cPhotoisomerization efficiency determined by UV-vis absorption data.

Interestingly, these molecules show luminescence after photoisomerization in contrast to common azobenzene derivatives (Figure 5). Upon UV irradiation at $\lambda = 300$ nm,

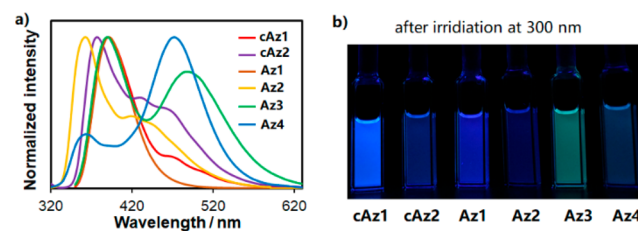


Figure 5. (a) Emission spectra of **cAz1**, **cAz2**, and **Az1–Az4** recorded in tetrahydrofuran (THF) ($c = 1.0 \times 10^{-5}$ M, $\lambda_{\text{ex}} = \lambda_{\text{abs(max)}}$) after the UV irradiation ($\lambda = 300$ nm). (b) Photographs of the emissive solutions in THF under UV lamp ($\lambda_{\text{ex}} = 365$ nm).

for example, a highly enhanced emission band quickly develops at 390 nm, with a remarkable increase in the fluorescence quantum efficiency from $\Phi < 1\%$ for **cAz1-Z** to 22% for **cAz1-E** (Table 1). The average fluorescence lifetimes (τ_{av}) were measured on the nanosecond scale after photoisomerization. To explore the fluorescence mechanism, we additionally investigated the photophysical properties of nonsubstituted diazocine and acyclic azobenzene for comparison with corresponding further functionalized derivatives. Although

the two parent systems show pronounced photochromism in their absorption spectra with characteristic optical responses (Figure S30 in the SI), almost no individual emission could be identified upon photoisomerization. Therefore, we conclude that the functionalization of π -extension with aryl fluorophore strongly contributes to the turn-on fluorescence, including triphenylamino and triarylborane moieties (Az1–Az4) and other groups.

To examine the responsive validity of diazocine-based materials, we compared the *cis*–*trans* isomerization rate and photochromic sensitivity. Previous studies on the *cis*–*trans* photoisomerization of azobenzenes have shown that the photoconversion follows the first-order kinetics and the rate constant k can be acquired from the equation

$$\ln \left[\frac{(A_0 - A_\infty)}{(A_t - A_\infty)} \right] = kt$$

where A_0 , A_t , and A_∞ are the absorbances before UV irradiation, at time t , and after irradiation for prolonged time, respectively.⁸ The forward isomerization absorption data were fitted into the equation for cAz2, Az2, and Az4 with similar π -conjugation length. As shown in Figure 6a, the derived

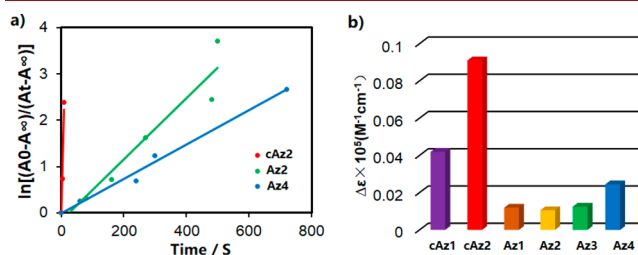


Figure 6. (a). Data fitting for comparison of the *cis*–*trans* isomerization rate based on the absorbances at $\lambda_{\text{abs(max)}}$ of the initial bands for cAz2, Az2, and Az4 with similar π -conjugation length. (b) Comparison of the photochromic sensitivity based on the absorbance changes at $\lambda_{\text{abs(max)}}$ of the new bands ($c = 1.0 \times 10^{-5}$ M, THF).

conversion rate constants (k) were found to be 2.4×10^{-1} s⁻¹ for cAz2, 6.6×10^{-3} s⁻¹ for Az2, and 3.7×10^{-3} s⁻¹ for Az4, indicative of a highly efficient photoswitching of cAz2. Data fitting of other molecules is shown in Figure S40 in the SI, and we found their k values to be 1.1×10^{-2} , 5.2×10^{-2} , and 1.1×10^{-2} s⁻¹ for cAz1, Az1, and Az3, respectively. We also inspected the absorbance difference upon the completion of photoisomerization (Figure 6b). A greater color change and more sensitive response were achieved for cAz1 and cAz2, with respect to other linear analogues. Hence, the diazocine-based molecular systems are superior in photochromic switches.

To evaluate the photostability of the fluorescence properties of these molecules, we chose cAz1 and cAz2 as representative examples and monitored the photoluminescence spectra (see Figure 7, as well as Figure S41 in the SI). Similar to the trend observed in ¹H NMR for cAz1, the highly enhanced emission after UV irradiation remains unchanged on the visible-light irradiation (e.g., at $\lambda = 410$ nm), and no fluorescence decay occurred over 10 days of exposure under ambient conditions. However, the new emission band at 390 nm was fully quenched after heating at 70 °C. These observations strongly suggest that the fluorescence “on” state of cAz1-*E* is light-tolerant and can only be switched back to the “dark” state of *Z* isomer in response to temperature T . No fatigue/degradation

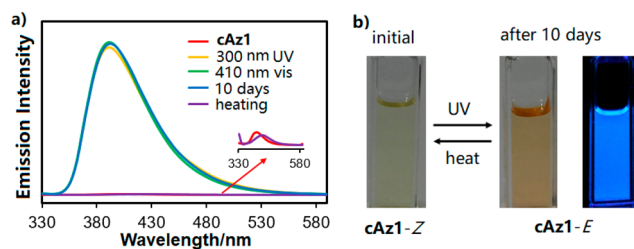


Figure 7. (a) Photoluminescence durability based on emission measurements for cAz1 in THF. Inset shows the expansion of the emission spectra before UV irradiation and after heating. (b) Photographs of the solution cAz1 in THF: before UV irradiation under ambient light (left, *Z*), after UV irradiation under ambient light (middle, *E*), and with irradiation using a UV hand lamp (right, *E*), respectively.

was observed in ¹H NMR over several cycles. A similar property was also deduced for cAz2 (see the SI). Such a phenomenon is in contrast to those of UV-vis photoswitching systems, which is of considerable advantage for sustainable light-emitting applications. The effective extension of π -conjugation may have a great impact on this.

In conclusion, we have successfully synthesized the first examples of conjugated photochromic materials based on the unique ring-constrained photoswitchable diazocine moieties. Spectroscopic studies elucidated that cAz1 and cAz2 undergo a faster photoswitching isomerization, in comparison to the parent azobenzene analogues, indicating that the diazocine-based molecular systems would ideally serve as highly efficient photochromic switches. Meanwhile, these molecules can persistently remain in the fluorescence “on” state rather than energy-transfer-induced luminescence quenching upon photoisomerization. Instead, the stable fluorescence can only be switched off via thermal quenching due to the back isomerization. We envision that the key findings on uncommon diazocines provide a proof of concept for the design of new light-emitting materials, based on multifunctional conjugated azobenzene derivatives.

■ ASSOCIATED CONTENT

Supporting Information

The Supporting Information is available free of charge on the ACS Publications website at DOI: 10.1021/acs.orglett.9b01215.

Experimental procedures, analytic data (¹H, ¹³C, ¹¹B, and MS) for all products and intermediates (PDF)

Accession Codes

CCDC 1902679, 1902683, and 1906983 contain the supplementary crystallographic data for this paper. These data can be obtained free of charge via www.ccdc.cam.ac.uk/data_request/cif, or by emailing data_request@ccdc.cam.ac.uk, or by contacting The Cambridge Crystallographic Data Centre, 12 Union Road, Cambridge CB2 1EZ, UK; fax: +44 1223 336033.

■ AUTHOR INFORMATION

Corresponding Author

*E-mail: pangkuan@bit.edu.cn.

ORCID

Suning Wang: 0000-0003-0889-251X

Pangkuan Chen: 0000-0002-8940-7418

Notes

The authors declare no competing financial interest.

ACKNOWLEDGMENTS

Q.Z., S.W., and P.C. thank the National Natural Science Foundation of China for financial support (Grant Nos. 21571017 and 21772012). We thank Prof. Nan Wang and Yun Li (Beijing Institute of Technology) for their help with XRD analysis. We thank the Analysis & Testing Centre at the Beijing Institute of Technology for advanced facilities.

REFERENCES

- (1) (a) Bertleson, R. C.; Maeda, S.; Van Gemert, B. In *Organic Photochromic and Thermochromic Compounds*, Vol. 1; Crano, J. C., Guglielmetti, R. J., Eds.; Plenum Press: New York, 1999. (b) Nigel Corns, S.; Partington, S. M.; Towns, A. D. *Color. Technol.* **2009**, *125*, 249. (c) Feringa, B. L.; Brown, W. R. *Molecular Switches*, 2nd Edition; Wiley-VCH: Weinheim, Germany, 2011.
- (2) *Intelligent Stimuli-Responsive Materials*; Li, Q.; Ed.; John Wiley & Sons: Hoboken, NJ, 2013.
- (3) (a) Russew, M. M.; Hecht, S. *Adv. Mater.* **2010**, *22*, 3348. (b) Saha, S.; Stoddart, J. F. *Chem. Soc. Rev.* **2007**, *36*, 77. (c) Fihey, A.; Perrier, A.; Browne, W. R.; Jacquemin, D. *Chem. Soc. Rev.* **2015**, *44*, 3719. (d) Szymanski, W.; Beierle, J. M.; Kistemaker, H. A. V.; Velema, W. A.; Feringa, B. L. *Chem. Rev.* **2013**, *113*, 6114.
- (4) Galanti, A.; Diez-Cabanes, V.; Santoro, J.; Valásek, M.; Minoia, A.; Mayor, M.; Cornil, J.; Samorì, P. *J. Am. Chem. Soc.* **2018**, *140*, 16062.
- (5) (a) Moreno, J.; Gerecke, M.; Grubert, L.; Kovalenko, S. A.; Hecht, S. *Angew. Chem., Int. Ed.* **2016**, *55*, 1544. (b) Bléger, D.; Schwarz, J.; Brouwer, A. M.; Hecht, S. *J. Am. Chem. Soc.* **2012**, *134*, 20597.
- (6) Hecht, S.; Bléger, D. *Angew. Chem., Int. Ed.* **2015**, *54*, 11338.
- (7) Zacharias, P. S.; Ameerunisha, S.; Korupoju, S. R. *J. Chem. Soc., Perkin Trans. 2* **1998**, *2*, 2055.
- (8) Surampudi, S. K.; Patel, H. R.; Nagarjuna, G.; Venkataraman, D. *Chem. Commun.* **2013**, *49*, 7519.
- (9) (a) Beharry, A. A.; Sadvovski, O.; Woolley, G. A. *J. Am. Chem. Soc.* **2011**, *133*, 19684. (b) Samanta, S.; Beharry, A. A.; Sadvovski, O.; McCormick, T. M.; Babalhavaeji, A.; Tropepe, V.; Woolley, G. A. *J. Am. Chem. Soc.* **2013**, *135*, 9777. (c) Dong, M.; Babalhavaeji, A.; Samanta, S.; Beharry, A. A.; Woolley, G. A. *Acc. Chem. Res.* **2015**, *48*, 2662.
- (10) (a) Yang, Y.; Hughes, R. P.; Aprahamian, I. *J. Am. Chem. Soc.* **2012**, *134*, 15221. (b) Yang, Y.; Hughes, R. P.; Aprahamian, I. *J. Am. Chem. Soc.* **2014**, *136*, 13190.
- (11) (a) Julià-López, A.; Hernando, J.; Ruiz-Molina, D.; González-Monje, P.; Sedó, J.; Roscini, C. *Angew. Chem., Int. Ed.* **2016**, *55*, 15044. (b) Perrier, A.; Maurel, F.; Jacquemin, D. *Acc. Chem. Res.* **2012**, *45*, 1173.
- (12) Siewertsen, R.; Neumann, H.; Buchheim-Stehn, B.; Herges, R.; Näther, C.; Renth, F.; Temps, F. *J. Am. Chem. Soc.* **2009**, *131*, 15594.
- (13) Samanta, S.; Qin, C.; Lough, A. J.; Woolley, G. A. *Angew. Chem., Int. Ed.* **2012**, *51*, 6452.
- (14) Hammerich, M.; Schütt, C.; Stähler, C.; Lentès, P.; Röhricht, F.; Höppner, R.; Herges, R. *J. Am. Chem. Soc.* **2016**, *138*, 13111.
- (15) (a) Cembran, A.; Bernardi, F.; Garavelli, M.; Gagliardi, L.; Orlandi, G. *J. Am. Chem. Soc.* **2004**, *126*, 3234. (b) Bandara, H. M. D.; Burdette, S. C. *Chem. Soc. Rev.* **2012**, *41*, 1809.
- (16) (a) Wakatsuki, Y.; Yamazaki, H.; Grutsch, P. A.; Santhanam, M.; Kutal, C. *J. Am. Chem. Soc.* **1985**, *107*, 8153. (b) Ghedini, M.; Pucci, D.; Calogero, G.; Barigelletti, F. *Chem. Phys. Lett.* **1997**, *267*, 341. (c) Babić, D.; Čurić, M.; Molčanov, K.; Ilc, G.; Plavec, J. *Inorg. Chem.* **2008**, *47*, 10446. (d) Srivastava, K.; Chakraborty, T.; Singh, H. B.; Butcher, R. J. *Dalton Trans* **2011**, *40*, 4489. (e) Bartwal, G.; Aggarwal, K.; Khurana, J. M. *New J. Chem.* **2018**, *42*, 2224.
- (17) (a) Yoshino, J.; Kano, N.; Kawashima, T. *Chem. Commun.* **2007**, 559. (b) Yoshino, J.; Kano, N.; Kawashima, T. *Chem. Lett.* **2008**, *37*, 960. (c) Yoshino, J.; Kano, N.; Kawashima, T. *Dalton Trans* **2013**, *42*, 15826. (d) Yoshino, J.; Furuta, A.; Kambe, T.; Itoi, H.; Kano, N.; Kawashima, T.; Ito, Y.; Asashima, M. *Chem. - Eur. J.* **2010**, *16*, 5026. (e) Kano, N.; Yamamura, M.; Kawashima, T. *Dalton Trans* **2015**, *44*, 16256.
- (18) Gon, M.; Tanaka, K.; Chujo, Y. *Angew. Chem., Int. Ed.* **2018**, *57*, 6546.
- (19) (a) Tsuda, K.; Dol, G. C.; Gensch, T.; Hofkens, J.; Latterini, L.; Weener, J. W.; Meijer, E. W.; De Schryver, F. C. *J. Am. Chem. Soc.* **2000**, *122*, 3445. (b) Han, M.; Hara, M. *J. Am. Chem. Soc.* **2005**, *127*, 10951.
- (20) Jacquart, A.; Williams, R. M.; Brouwer, A. M.; Ishow, E. *Chem. - Eur. J.* **2012**, *18*, 3706.